

Print ISSN

1110-7642

Online ISSN 2735-5039

AIN SHAMS DENTAL JOURNAL

Official Publication of Ain Shams Dental School June2025 • Vol. 38

The Effect of CBCT Voxel Size on Detection of Horizontal Root Fracture: An Ex-Vivo study

Ahmed Reda Rabea Yousef¹, Mostafa Saad-Eldin Ashmawy¹ Walaa Hussein Abu El-Ela¹

Aim: To assess the impact of cone-beam computed tomography (CBCT) voxel size on the observers' ability to detect horizontal root fracture.

Materials and methods: One hundred and four extracted posterior teeth with sound roots were prepared to have root canal filling (RCF). The teeth were then divided equally into four groups: RCF only, RCF with simulated horizontal root fracture (HRF), RCF and metallic post, and RCF with post and HRF. The teeth were randomly distributed and adapted into sockets of dry skull and mandible. Each assembly was scanned by two CBCT machines and two voxel sizes for each. Two oral radiologists assessed the images for HRF detection using a five-confidence scale. Sensitivity, specificity, and accuracy were measured.

Results: Inter-observer reliability ranged from very good to excellent. There was an excellent intra-observer agreement. Gendex machine images (0.2- and 0.08-mm voxel sizes) were more sensitive and accurate for fracture detection while i-CAT® images (0.2- and 0.125-mm voxel sizes) were more specific in sound roots identification. However, both machines and voxel sizes revealed significantly high diagnostic performance in HRF detection. The presence of intracanal metallic post resulted in higher accuracy compared to presence of RCF only but without a significant difference.

Conclusion: Consider using the large voxel size of both machines which provide appropriate accuracy for fracture detection and saving patient form excess x-radiation.

Keywords: Horizontal root fracture, CBCT, Voxel size, Root canal treatment.

 Ain Shams University, Faculty of Dentistry, Department of Oral and Maxillofacial Radiology, Cairo, Egypt. Corresponding author: Ahmed Reda Rabea Yousef, email: ahmedyousef@dent.asu.edu.eg

Introduction

Endodontically treated teeth have a lower resistance and a higher risk of fracture than healthy teeth. The root fracture may be either vertical or horizontal.^{2,3} Vertical root fracture (VRF) is a longitudinal fracture involving the cementum, dentine, and root canal system of a root.^{4,5} During endodontic treatment and post insertion, iatrogenic VRF commonly occurs. It also occurs in 2-5% of crown/root fracture cases.6 Horizontal root fracture (HRF) is a fracture line that runs transversely or obliquely across the long axis of the root. In anterior teeth, HRF occurs due to direct trauma especially in young adults while in posterior teeth, it typically happens due to indirect trauma during compaction of intracanal posts and root filling materials.²

Conventional radiographic detection of HRF depends on the direction of fracture line and its position. Transverse fractures in the cervical third of the root are detected in the standard 90° intraoral periapical film. Oblique fractures in the middle and apical thirds may require two additional intra-oral periapical radiographs at +/- 15° from the original, or an occlusal film to confirm the fracture line^{8,9} As the conventional radiograph is a two-dimensional (2D) representation of a three-dimensional (3D) object, the fracture line is more likely to be visible when the central ray is parallel to the fracture plane. 10

Nowadays, cone-beam computed tomography (CBCT) is the most widely imaging. available 3D It eliminates superimpositions and allows for visualization of the third dimension.¹¹ Moreover, small field of view (FOV) CBCT allows more accurate detection of dentoalveolar trauma periapical radiograph than due superimposition and difficulty to differentiate a root fracture from an overlapping alveolar process fracture. 12 However, presence of high-density materials: root canal filling (RCF). metallic posts¹³, restorative

materials¹⁴, and dental implants, may induce beam hardening artifacts in CBCT images. These artifacts might affect the diagnostic accuracy of CBCT.

Different CBCT systems provide variable image quality and diagnostic capacity. These systems differ in detector design, patient scanning settings, and data acquisitions parameters (FOV, voxel size, basis projection number, mA, kVp). 15,16 Several studies have compared the diagnostic accuracy of CBCT scans in the detection of VRF at different voxel resolutions. 17–19 However, few studies have evaluated CBCT with different parameters in detection of HRF. Costa et al, evaluated the effect of small and large FOV CBCT images on detection of HRF in presence and absence of intracanal metallic post. They reported that large volume CBCT images resulted in low accuracy in the detection of HRF specially in the presence of intracanal metallic post. 20,21 Wenzel et al.²² reported that i-CAT® CBCT images of 0.125 mm voxel size presented the highest sensitivity (87%) followed by periapical PSP images (74%) then CBCT images of 0.25 mm voxel size (72%). Therefore, the present study aimed to evaluate the effect of different voxel sizes of two CBCT systems on the observer's ability to detect simulated HRF in presence RCF only and RCF with a metallic post.

Material and Methods

An ex-vivo study was exempted from review by the research Ethics Committee of the Faculty of Dentistry, Ain Shams University (FDASU-Rec EM012304). Based on the results obtained by a previous study²¹, power analysis was done using an alpha error 0.05 and power of 80%. Estimated sample size was one hundred and four teeth.

Teeth selection and preparation

A total of one hundred and four human extracted maxillary and mandibular

premolars and molars were obtained from the oral surgery department. The teeth were examined visually using a macro lens under good lighting condition to ensure sound roots without any cracks or fractures. The root canals of all teeth were mechanically prepared using Fanta AF Blue rotary system file (Fanta dental material, shanghai, China). All root canals were then obturated with Gutta percha (Meta biomed co., ltd, Korea) using the lateral condensation technique and adseal sealer (Meta biomed co., ltd, Korea). Randomly, we select fifty-two teeth to receive a uni-metric metallic post (Dentsply, maillefer, Switzerland) inserted in the canals after removing two third of gutta percha from the palatal canal of upper teeth and distal canal of lower teeth.

Horizontal root fracture simulation

We used a diamond disc (SS white, USA) with 19 mm diameter and 0.13 mm thickness to perform an artificial horizontal fracture in 26 teeth with RCF only and 26 teeth with RCF and post. The fracture line runs from the outer surface of the root to touch the gutta percha in a horizontal manner. As a result, we obtained four groups of sample teeth, each one contains 26 premolar and molars. The first had RCF only, the second had RCF with HRF, the third had RCF with post, and the fourth had RCF with post and HRF. The teeth were color coded and only the primary investigator had the key. CBCT image acquisition

For CBCT imaging, the teeth were randomly distributed and adapted into sockets of dry skull and mandible using 0.3-mm layer of utility wax (Tenatex Red; Kemdent, Swindon, UK) sequentially. The teeth were arranged in quadrants; each quadrant received two premolars and two molars, summing up eight teeth per arch (maxilla or mandible). Thus the 104 posterior teeth were placed in thirteen arches assembly (seven mandibles and six maxillae).

Each arch assembly was scanned by two CBCT machines using two different imaging protocols for each (Fig 1).

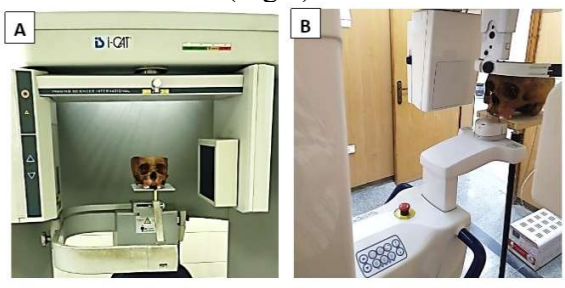


Figure 1: CBCT scanning of the maxillary arch using i-CAT® (A) and Gendex DP-800 machines (B).

First, CBCT scanning with i-CAT® next generation (Imaging Sciences International, Hatfield, PA) working at 120 kVp, 5 mA and exposure time 26.9 second. Each arch was scanned twice; one scan using 0.125 mm voxel and 4*16 cm FOV and second scan using 0.2 mm voxel and 6*16 cm FOV. Second, CBCT scanning using Gendex DP-800 (PaloDX Group Oy Finland). For using 0.2 mm voxel, a full arch scan was obtained using 90 kVp, 6.3 mA, exposure time 6.1seconds and 7.8*7.8 cm FOV. For using 0.08 mm voxel, two segments' scans (right and left side) were acquired using 90 kVp, 6.3 mA, exposure time 8.7 seconds and 5*5 cm FOV. Finally, we obtained five scans for each arch: three scans using Gendex (0.08 mm voxel for right segment, 0.08 mm voxel for left segment and 0.2 mm voxel for full arch) and two full arch scans using i-CAT® with 0.2mm and 0.125 mm voxel sizes.

Digital Imaging and Communications in Medicine (DICOM) images were transferred to a third party OnDemand3D software (Cybermed, Seoul, South Korea). For standardization, the primary investigator adjusted all the images with 0.1 mm thickness and 1 mm slice interval. Moreover, each scan was coded, so the observers were blinded to the machine type and the voxel size. Two oral radiologists with ten years' experience were calibrated to evaluate the axial, coronal and

sagittal tomographic slices for absence or presence of HRF in each root using a five-point scale of confidence:1. definitely absent, 2. probably absent, 3. not sure, 4. probably present, 5. definitely present ²³ The observers were allowed to adjust image clarity (density, contrast, and sharpness) and move freely across the cuts. Twenty percent of the sample teeth were assessed twice by the two observers with two weeks interval. Fig.2 shows example images for each CBCT machine and each voxel size.

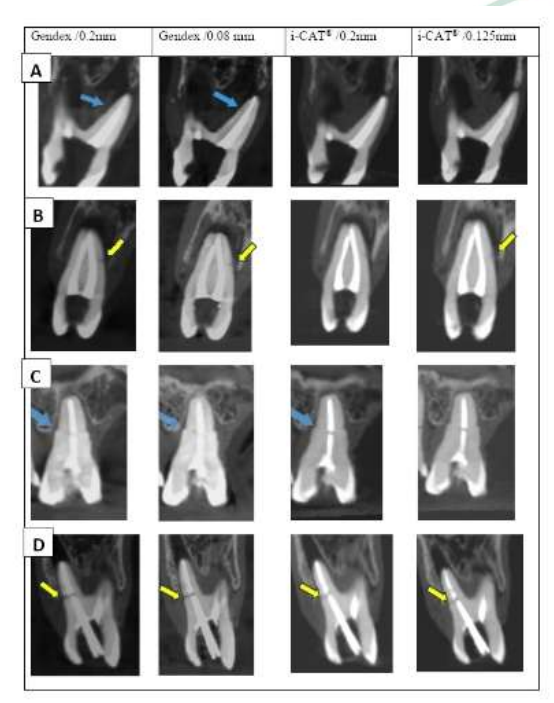


Figure 2: (A) shows coronal images of a molar with root canal treatment and sound root. Gendex images showed pseudo fracture lines (blue arrows). (B) shows coronal images of a premolar with root canal treatment and HRF which is clearly defined in images of Gendex and i-CAT® image of 0.125 mm (yellow arrows). (C) shows coronal images of a premolar with root canal treatment, metallic post and sound root. Gendex images showed a thin radiolucent line artifact from the metallic post simulating a HRF (the blue arrows). (D) shows coronal images of a molar with root canal treatment, post and HRF. The fracture line is defined in all images, and it was more obvious in Gendex 0.08mm voxel image than others (yellow arrows).

Statistical analysis

The recorded data were analyzed using the Statistical Package for Social Sciences SPSS® version 23.0 (IBM Corporation, NY, USA). Inter- and intra-observer reliability were measured by Intraclass Correlation Coefficient (ICC) analysis and interpreted as: < 0.10 no agreement, 0.10-0.40 poor, 0.41-0.60 good, 0.61-0.80 very good, and 0.81excellent agreement. Sensitivity, Specificity and Accuracy of HRF detection by each CBCT and voxel size were calculated. The diagnostic accuracy of both machines and all used voxels were compared using fisher's exact test. P-value < 0.05 was considered significant. P-value <0.001 was considered as highly significant. P-value >0.05 was considered insignificant.

Results

The inter-observer reliability adapted according to voxel size of assessed image. A very good interobserver reliability (0.73 - 0.76) was obtained when interpreting images of 0.2 mm voxel size of the two machines. While there was an excellent agreement between observers (0.92 - 0.95) when interpreting images of i-CAT® 0.125 and Gendex 0.08 mm (Table 1).

Table 1: Intraclass Correlation Coefficient (ICC) values of inter-observer agreement for each reading

1 000 001112							
CBCT/	Inter-observer reliability						
Voxel size (mm)	Reading	one	Reading two				
,	ICC (95% CI)	P-value	ICC (95% CI)	P-value			
i-CAT®/ 0.2	1.000 (1.00-1.00)	<0.001**	0.738 (0.40-0.89)	0.002*			
Gendex / 0.2	0.764 (0.32-0.92)	0.004*	1.000 (1.00-1.00)	<0.001**			
i-CAT® /0.125	1.000 (1.00-1.00)	<0.001**	1.000 (1.00-1.00)	<0.001**			
Gendex / 0.08	0.921 (0.83-0.96)	<0.001**	0.958 (0.90-0.98)	<0.001**			

*p-value $\!<\!0.05$ is significant, **p-value $\!<\!0.001$ is highly significant

There was an excellent intra-observer agreement for detection of HRF with all used voxel sizes (0.91 - 0.98) and both observers (Table 2).

Table 2: Intraclass Correlation Coefficient (ICC) values of intra-observer agreement

values of intra-observer agreement							
CDCT / VI	Intra-observer reliability						
CBCT / Voxel size (mm)	Observer	one	Observer two				
	ICC (95% CI)	P-value	ICC (95% CI)	P-value			
i-CAT®/ 0.2	0.962 (0.94-0.97)	<0.001**	0.918 (0.88-0.95)	<0.001**			
Gendex / 0.2	0.960 (0.94-0.97)	<0.001**	0.970 (0.96-0.98)	<0.001**			
i-CAT® /0.125	0.962 (0.94-0.97)	<0.001**	0.980 (0.97-0.99)	<0.001**			
Gendex / 0.08	0.960 (0.94-0.97)	<0.001**	0.970 (0.96-0.98)	<0.001**			

*p-value < 0.05 is significant, **p-value <0.001 is highly significant

Table 3 shows that images of both CBCT machines and voxel sizes presented significant sensitivity, specificity, and accuracy in detection of HRF in presence or absence of metallic post. Gendex machine images (0.2- and 0.08-mm voxel sizes) were more sensitive and accurate for fracture detection while i-CAT® images (0.2- and 0.125-mm voxel sizes) were more specific in sound roots identification.

Table 3: Sensitivity, specificity, and accuracy for horizontal root fracture detection through CBCT yoxel sizes.

		CDU	1 10	xei siz	es.						
		i-CAT	® 0.2	i-CAT(₿ 0.125	Gend	lex 0.2	Gende	1	P-value	
		Observe r 1	Observer 2	Observer 1	Observe r 2	Observe r 1	Observe r 2	Observe r 1	Observe r 2		
Sensitivity	G 1&2	96%	82%	89%	96%	96%	100%	93%	93%	<0.001*	1
	G 3&4	89%	96%	96%	100%	100%	96%	100%	100%	<0.001* *	
	G 1&2	100%	96%	100%	100%	96%	96%	96%	100%	<0.001*	
Specificity	G 3&4	100%	96%	100%	96%	96%	94%	96%	96%	<0.001* *	
Accuracy	G 1&2	98%	89%	94%	98%	96%	98%	94%	96%	<0.001* *	
Accuracy	G 3&4	94%	96%	98%	98%	96%	96%	98%	98%	<0.001*	
PPV	G 1&2	100%	96%	100%	100%	96%	96%	96%	100%	<0.001* *	
	G 3&4	100%	96%	100%	96%	93%	96%	96%	96%	<0.001* *	
NPV	G 1&2	96%	83%	90%	96%	96%	100%	93%	92%	<0.001* *	
NEV	G 3&4	89%	96%	96%	100%	100%	96%	100%	100%	<0.001* *	

**p-value <0.001 is highly significant accuracy. PPV: Positive predictive value; NPV: Negative predictive value. G 1(RCF only), G 2 (RCF with HRF) G 3, (RCF with post), G 4 (RCF with post and HRF)

Compared to the presence of RCF only, accuracy of fracture detection increased with presence of intracanal metallic post in both machines and voxel sizes. However, the differences were not statistically significant (Table 4).

Table 4: Fisher's exact test comparing accuracy of CBCT-based detection of horizontal root fracture in presence of root canal filling only and presence of RCF with post.

CBCT / Voxel size (mm)	Accuracy (%) In presence of RCF only	Accuracy (%) In presence of RCF and post	p-value
i-CAT® / 0.2	89 - 98	94 - 96	0.145- 0.056
i-CAT® / 0.125	94 - 98	98	0.175 - 0.959
Gendex / 0.2	96 - 98	96	0.971 - 0.401
Gendex / 0.08	94 - 96	98	0.175 - 0.449

RCF: Root canal filling

Discussion

HRF can either be transverse or oblique, single, or multiple, complete, or incomplete. The diagnosis of incomplete root fracture is time-consuming and difficult especially when using a periapical radiograph. ^{24,25} So, CBCT technology is the appropriate solution in such instances since it allows the dentists to monitor a region in three separate planes and obtain 3D data. ²⁵

Smaller voxel sizes (i-CAT® 0.125 mm and Gendex 0.08 mm) consistently resulted in high inter- and intra-observer reliability. This could be attributed to more detailed and clear images of small voxel sizes, leading to more consistent interpretations. Variability in inter-observer reliability, especially with larger voxel sizes, highlights the need for standardized training and calibration protocols. Ensuring that all observers are equally skilled and interpret the images similarly can reduce variability.

For i-CAT® machine, assessment of HRF was more sensitive, specific, and accurate when using images of 0.125 mm voxel than 0.2 mm voxel, but the differences were not significant. Similarly, Ozer et al and da Silveira et al. 17,18 reported that no significant

difference in the accuracy of VRFs detection using CBCT images of 0.125- and 0.4-mm voxel sizes. On contrary, Uysal et al.²⁶ reported that high-resolution CBCT images yielded higher sensitivity and specificity for detecting **VRFs** than lower-resolution images. Moreover, Wenzel et al.27, found that high-resolution i-CAT® CBCT images (0.125 mm voxel size) presented the highest sensitivity (87%) followed by periapical PSP images (74%) then the lower-resolution CBCT images 0.25 mm voxel size (72%) and the differences between CBCT in high and lower resolution images were highly significant.

In the present study i-CAT® CBCT images allowed slightly better specificity of sound root detection than Gendex machine images. This may suggest better dealing of i-CAT® machine with the artifacts. However, Gendex machine outperformed i-CAT® machine in sensitivity and accuracy in horizontal fracture detection. This may be due to the proportional relationship between FOV and voxel size of Gendex CBCT machine (FOV 5*5/0.08 mm voxel and FOV 7.8*7.8/0.2 mm voxel) compared to (FOV 4*16/0.125mm voxel and FOV 6*16/0.2 mm voxel) of i-CAT® CBCT machine. Increasing the FOV increases the scatter radiation, image noise, and decreases detection accuracy. Similarly, Salineiro et al compared four different imaging protocols of i-CAT® machine in the detection of HRF.²⁸ They concluded that both 6x16/0.25 mm and 8x8/0.20 mm imaging protocols produced higher sensitivity, specificity, and accuracy than 6x16/0.2 mm and 8X8 cm/0.25 mm voxel imaging protocols.

Compared to presence of root filling only, presence of metallic post slightly increased the sensitivity and accuracy and decreased specificity but without significant difference. Likely, Zhang JH et al studied the effect of various intracanal materials on diagnostic accuracy of CBCT in detection of

VRF. They found that the influence of fiber posts, gutta-percha points, and titanium posts was not significant, whereas the influence of gold-palladium posts was significant.²⁹ Moreover, Costa et al.²¹ and Bechara et al.³⁰ reported that absence of the metallic post increases the specificity. Similarly, Jakobson et al reported that CBCT had a higher sensitivity for root fracture diagnosis in roots with posts and buccolingual fractures. They also found that sensitivity of i-CAT® CBCT machine using 0.2 mm was 96.25% in groups with intracanal metallic post and deceased to 93.25 % in groups without post.^{31,32} contrary, Costa et al.²¹ and Menezes et al.³³ concluded that presence of post decreased accuracy of root fracture detection using CBCT. This difference could be due to different post materials; in the current study we used a titanium post compared to the cobalt chromium alloy post used in their studies. Titanium posts produce lesser artifact than cobalt chromium alloy due to the difference in the atomic number and presence of metals with higher atomic numbers in cobalt-chromium alloys (e.g., molybdenum and tungsten).³⁴

One of the limitations of the present study was the ex-vivo design which removed artifacts from patient motion. However, this design allows studying different imaging protocols without harmful effect on the patients. In addition, the artificially created fracture line was more well-defined than the natural one. Thus, detection of natural horizontal root fracture in vivo may produce variable results.

Conclusion

Both CBCT machines and voxel sizes produced significantly high diagnostic performance for HRF detection. Gendex machine outperformed i-CAT® machine in sensitivity and accuracy due to its smaller FOV and decreased scattering radiation. Moreover, the presence of intracanal titanium

metallic post had no significant effect on the detection accuracy of HRF across all voxel sizes and CBCT machines.

Funding

This research article received no external funding and was totally funded by the authors.

Data availability

The datasets used and/or analyzed during the current study are available from the corresponding author upon reasonable request.

Ethics approval and consent to participate

The research approved by Ethics Committee of the Faculty of Dentistry, Ain Shams University number (FDASU-Rec EM012304).

Competing interests

The authors declare that they have no conflict of interest.

References

- 1. Marchionatti, A. M. E., Wandscher, V. F., Rippe, M. P., Kaizer, O. B. & Valandro, L. F. Clinical performance and failure modes of pulpless teeth restored with posts: a systematic review. *Braz Oral Res* **31**, e64 (2017).
- 2. Malhotra, N., Kundabala, M. & Acharaya, S. R. A review of root fractures: diagnosis, treatment and prognosis. *Dent Update* **38**, (2011).
- 3. Majorana, A., Pasini, S., Bardellini, E. & Keller, E. Clinical and epidemiological study of traumatic root fractures. *Dent Traumatol* **18**, 77–80 (2002).
- 4. Luebke, R. G. Vertical crown-root fractures in posterior teeth. *Dent Clin North Am* **28**, 883–94 (1984).
- 5. Patel, S., Bhuva, B. & Bose, R. Present status and future directions: vertical root fractures in root filled teeth. *Int Endod J* **55 Suppl 3**, 804–826 (2022).
- 6. Andreasen, J. O., Andreasen, F. M., Skeie, A., Hjørting-Hansen, E. & Schwartz, O. Effect of treatment delay upon pulp and periodontal healing of traumatic dental injuries A review article. *Dental Traumatology* vol. 18 116–128 Preprint at https://doi.org/10.1034/j.1600-9657.2002.00079.x (2002).

- 7. Tsai, Y. -L. *et al.* Horizontal root fractures in posterior teeth without dental trauma: tooth/root distribution and clinical characteristics. *Int Endod J* **50**, 830–835 (2017).
- 8. Ranka, M., Shah, J. & Youngson, C. Root fracture and its management. *Dent Update* **39**, 530–2, 535–8 (2012).
- 9. Flores, M., Holan, G., Andreasen, J. & Lauridsen, E. Injuries to the primary dentition. In: Andreasen JO, Andreasen FM, Andersson L, editors. Textbook and color atlas of traumatic injuries to the teeth, 5th edn. Copenhagen, Denmark: Wiley Blackwell. 556–88 (2019).
- 10. Loubele, M. *et al.* Image quality vs radiation dose of four cone beam computed tomography scanners. *Dentomaxillofac Radiol* **37**, 309–18 (2008).
- 11. Cohenca, N., Simon, J. H., Roges, R., Morag, Y. & Malfaz, J. M. Clinical indications for digital imaging in dento-alveolar trauma. Part 1: traumatic injuries. *Dent Traumatol* 23, 95–104 (2007).
- 12. Mallya, S. M. & Diplomate, P. White and Pharoah's Oral Radiology Principles and Interpretation 8TH EDITION.
- 13. Costa, F. F. *et al.* Influence of cone-beam computed tomographic scan mode for detection of horizontal root fracture. *J Endod* **40**, 1472–6 (2014).
- 14. Brito-Júnior, M., Santos, L. A. N., Faria-e-Silva, A. L., Pereira, R. D. & Sousa-Neto, M. D. Ex vivo evaluation of artifacts mimicking fracture lines on cone-beam computed tomography produced by different root canal sealers. *Int Endod J* 47, 26–31 (2014).
- 15. Mischkowski, R. A. *et al.* Diagnostic quality of multiplanar reformations obtained with a newly developed cone beam device for maxillofacial imaging. *Dentomaxillofacial Radiology* **37**, 1–9 (2008).
- 16. Mozzo, P., Procacci, C., Tacconi, A., Tinazzi Martini, P. & Bergamo Andreis, I. A. A new volumetric CT machine for dental imaging based on the cone-beam technique: preliminary results. *Eur Radiol* **8**, 1558–1564 (1998).
- 17. Yiit Özer, S. Detection of vertical root fractures by using cone beam computed tomography with variable voxel sizes in an in vitro model. *J Endod* **37**, 75–79 (2011).
- 18. da Silveira, P. F. *et al.* Detection of vertical root fractures by conventional radiographic examination and cone beam computed tomography an in vitro analysis. *Dent Traumatol* **29**, 41–6 (2013).
- 19. Melo, S. L. S., Bortoluzzi, E. A., Abreu, M., Corrêa, L. R. & Corrêa, M. Diagnostic ability of a cone-beam computed tomography scan to assess longitudinal root fractures in prosthetically treated teeth. *J Endod* **36**, 1879–1882 (2010).

- 20. Costa, F. F. *et al.* Use of Large-volume Cone-Beam Computed Tomography in Identification and Localization of Horizontal Root Fracture in the Presence and Absence of Intracanal Metallic Post. *J Endod* **38**, 856–859 (2012).
- 21. Costa, F. F., Gaia, B. F., Umetsubo, O. S. & Paraiso Cavalcanti, M. G. Detection of horizontal root fracture with small-volume cone-beam computed tomography in the presence and absence of intracanal metallic post. *J Endod* 37, 1456–1459 (2011).
- 22. Wenzel, A., Haiter-Neto, F., Frydenberg, M. & Kirkevang, L. L. Variable-resolution cone-beam computerized tomography with enhancement filtration compared with intraoral photostimulable phosphor radiography in detection of transverse root fractures in an in vitro model. *Oral Surg Oral Med Oral Pathol Oral Radiol Endod* 108, 939–945 (2009).
- 23. Andraws Yalda, F. *et al.* Determination of a conebeam CT low-dose protocol for root fracture diagnosis in non-endodontically treated anterior maxillary teeth. *Dentomaxillofac Radiol* 51, 20210138 (2022).
- 24. Parekh, D. J., Sathyanarayanan, R. & Manjunath, M. T. Clinical management of mid-root fracture in maxillary central incisors: case reports. *Int J Oral Sci* **2**, 215–21 (2010).
- 25. Chute, A. K., Toshniwal, A., Gade, V. & Chute, M. Repair of incomplete horizontal mid-root fracture of maxillary central incisor with mineral trioxide aggregate: A follow up report. *J Conserv Dent* 17, 393–5 (2014).
- Uysal, S., Akcicek, G., Yalcin, E. D., Tuncel, B.
 Dural, S. The influence of voxel size and artifact reduction on the detection of vertical root fracture in endodontically treated teeth. *Acta Odontol Scand* 79, 354–358 (2021).
- 27. Wenzel, A., Haiter-Neto, F., Frydenberg, M. & Kirkevang, L.-L. Variable-resolution cone-beam computerized tomography with enhancement filtration compared with intraoral photostimulable phosphor radiography in detection of transverse root fractures in an in vitro model. *Oral Surg Oral Med Oral Pathol Oral Radiol Endod* 108, 939–45 (2009).
- 28. SALINEIRO, F. C. S., PINHEIRO, L. R., SANTOS JÚNIOR, O. dos & CAVALCANTI, M. G. P. Detection of horizontal root fracture using four different protocols of cone-beam computed tomography. *Braz Oral Res* **29**, 1–6 (2015).
- 29. Zhang, J. H., Pan, J., Sun, Z. P. & Wang, X. [Effect of various intracanal materials on the diagnostic accuracy of cone-beam computed tomography in vertical root fractures]. *Beijing da xue xue bao. Yi xue ban = Journal of Peking University. Health sciences* **55**, 333–338 (2023).

- 30. Bechara, B. *et al.* Contrast-to-noise ratio difference in small field of view cone beam computed tomography machines. *J Oral Sci* **54**, 227–232 (2012).
- 31. Jakobson, S. J. M. *et al.* The influence of metallic posts in the detection of vertical root fractures using different imaging examinations. *Dentomaxillofac Radiol* **43**, 20130287 (2014).
- 32. Mohammadpour, M. et al. Effect of titanium and stainless steel posts in detection of vertical root fractures using NewTom VG cone beam computed tomography system. *Imaging Sci Dent* 44, 89 (2014).
- 33. Menezes, R. F. de *et al.* Detection of vertical root fractures in endodontically treated teeth in the absence and in the presence of metal post by conebeam computed tomography. *BMC Oral Health* 16, 48 (2016).
- 34. Panjnoush, M. et al. Effect of Exposure Parameters on Metal Artifacts in Cone Beam Computed Tomography. J Dent (Tehran) 13, 143–150 (2016).

Journal